Dyes and Pigments 86 (2010) 271–277

Contents lists available at ScienceDirect

Dyes and Pigments

journal homepage: www.elsevier.com/locate/dyepig

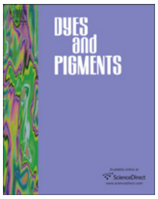

# Colorimetric properties of reversible thermochromic printing inks

Rahela Kulčar [a], Mojca Friškovec [b], Nina Hauptman [c], Alenka Vesel [d], Marta Klanjšek Gunde [c,*]

[a] University of Zagreb, Faculty of Graphic Arts, Getaldićeva 2, Zagreb, Croatia
[b] Cetis, Graphic and Documentation Services, d.d., Čopova 24, Celje, Slovenia
[c] National Institute of Chemistry, Ljubljana, Hajdrihova 19, Slovenia
[d] «Jožef Stefan» Institute, Ljubljana, Jamova 39, Slovenia

ARTICLE INFO

*Article history:*
Received 6 January 2010
Received in revised form
22 January 2010
Accepted 23 January 2010
Available online 1 February 2010

*Keywords:*
Thermochromism
Thermochromic printing inks
Microcapsules
Colorimetry
Hysteresis
Reversibility

ABSTRACT

The colorimetric properties of three, leuco dye-based thermochromic inks at 31 °C activation temperature were studied. The inks had similar pigment particle size distribution and comparably thick microcapsule shells with similar stability against oxygen plasma etching. The colour of the inks was dependent on temperature as well as the thermal history of the sample, which gives rise to colour hysteresis. The area of the observed hysteresis loop in CIELAB colour space determines how different colours appear on the sample when decolourisation and colourisation processes are compared. The largest colour difference achieved for the same sample that arose because of different thermal history and temperature were determined. Four characteristic temperatures were ascribed to the two chemical reactions causing colour hysteresis. The stability of the decolourised state at cooling $<$activation temperature was confirmed as $>$10 h. The reversibility of the thermochromic effect diminished approximately linearly with the highest heating temperature.

## 1. Introduction

Thermochromic (TC) materials respond to changes of temperature by colour change [1]. Thermochromic printing inks have become increasingly important for various applications in graphic art such as smart packaging, security printing and marketing activities in which value or uniqueness of a product is desired [2–5]. The colour properties of such inks are based on chromogenic functional polymers rather than inorganic thermochromic pigments; as organic compositions can be made in many colours and which display colour change at desired temperatures, organic systems are almost exclusively used in printing inks [1].

Reversible thermochromic organic materials usually consist of at least three components namely a colour former, colour developer and solvent. Common colour formers are electron-donating, leuco dyes, as exemplified by spirolacones, fluorans, spiropyrans or fulgides. As these compounds change colour when pH is altered, they are in reality, halochromic. Frequently used examples include crystal violet lactone and thymolphthalein. Their reaction with the second component, the electron-accepting developer, defines the position of the longest wavelength absorption which causes colouration/decolouration. Frequently used developers are typically weak acids such as bisphenol A, gallates, phenols, hydroxybenzoates and hydroxycoumarin derivatives. The melting point of the solvent controls the temperature at which the colour of the three-phase composite, thermochromic changes. Whilst several polar solvents are reported to be suitable, alcohols and esters seems to be preferred [6–17].

Reversible colour change occurs via two competing reactions namely that between dye and developer and the other between solvent and developer. The first of these interactions prevails at lower temperatures where the solvent exists in its solid form and gives rise to coloured dye–developer complexes; at higher temperature the solvent melts, causing the solvent–developer interaction to dominate. Thus, dye–developer complexes are destroyed which converts the system into its colourless state [6–12]. Leuco dye–developer–solvent composites are by far the most important systems to achieve thermochromic properties using organic materials [1]. The temperature at which decolourisation/colourisation occurs is controlled by the melting temperature of the solvent. Several definitions of this temperature are used in the literature, such as switching [11], decolourisation [6,7] or activation temperature [5]; in this study the term activation temperature ($T_A$) is used.

A three component organic thermochromic composite (leuco dye–developer–solvent) must be optimised to order to secure high

---

* Corresponding author. Tel.: +386 1 476 0200; fax: +386 1 476 0300.
*E-mail address:* marta.k.gunde@ki.si (M.K. Gunde).

0143-7208/$ – see front matter © 2010 Elsevier Ltd. All rights reserved.
doi:10.1016/j.dyepig.2010.01.014

colour contrast between the two states (colourless and coloured), reasonable colour stability in both equilibrium states and quick response to temperature [7,9–13]. The range of possible applications of such thermochromic material is markedly enlarged by the use of microencapsulation to protect the system from unwanted reactions with their surroundings. Each microcapsule, or so-called leuco dye pigment, contains the entire system required to reproduce the colour. The microencapsulation process provides spherical microcapsules $\leq 20\ \mu$m. Some crystals of non-encapsulated composite can remain in the resulting powder [11]. Microcapsules must withstand standard mixing and application procedures.

A thermochromic printing ink is a mixture of thermochromic pigments and a binder. Each component constitutes a separate phase and it is supposed that these do not influence each other. The microcapsules are not inert and display negligible light scattering; their size ranges are typically 3–5 μm which is >10-times larger than conventional pigment particles. The decolourisation/colourisation reactions are regarded to be reversible and it is believed that the process can be repeated several thousand times [2]. Although leuco dye-based thermochromic inks of various activation temperatures are available, from −15 °C up to 65 °C, most applications are limited to three standard temperature ranges, namely cold (∼10 °C), body-heat activated (∼31 °C) and warm (∼43 °C) [18]. All major ink types such as water-based and photocuring for application on paper, plastics and textile are available.

Despite the relatively well known functionality of thermochromic leuco dye-based inks, very little has been published about their colorimetric characteristics [5]. These are of significance from an application perspective [1] in which context, the most important characteristics are the temperature-dependent properties of the complex thermochromic system, the degree of its reversibility and factors that influence this. This paper concerns the colorimetric properties of red, blue and black, leuco dye-based thermochromic inks with an activation temperature of 31 °C. Special attention was devoted to the colorimetric properties that describe colour hysteresis and the influence of temperatures in excess of the activation temperature on the reversibility of the thermochromic process.

## 2. Experimental

UV-curable TC screen printing inks UV TCX (Coates Screen Inks GmbH, Germany) in red (UV TCX R-31), blue (UV TCX B-31) and black (UV TCX N-31) shades were used, which comprised an acrylate UV-curable vehicle and leuco dye thermochromic pigments with an activation temperature of 31 °C (according to the maker's specification). The thermochromic pigment particles in the wet ink were characterized using the Fineness-of-Grind Gauge (Byk-Gardner, Germany) to obtain the size of the largest particles.

The inks were screen-printed over OBA-free gloss coated paper (150 g/m$^2$) using a flatprinting SD 05 machine (RokuPrint Germany) employing SEFAR® PET 1500 high-modulus monofilament polyester mesh 120/34Y. The printed samples were cured using a UV dryer Aktiprint L (Technigraf, Germany) employing UV energy of approximately 0,83 W cm$^{-2}$ at 8 m min$^{-1}$, the curing energy at the sample surface being ∼400 mJ/cm$^2$ as measured using a UV integrator (Technigraf, Germany). The thickness of the dry layers was measured using a Talysurf (Rank Taylor Hobson Series 2).

The particle size distribution was determined by image analysis of optical micrographs. For this purpose a very thin film of ink was prepared on a glass slice and UV-cured. The dry layers weremonitored by optical microscope in bright and dark field. The micrographs were quantified using *Image-J* public domain software.

The thermochromic pigment particles were analysed using a Karl Zeiss Supra 35 field emission SEM. As only the particles located at the very top of a dry screen-printed sample could be observed, more particles were made visible when the topmost layer of the binder was selectively etched by weakly ionised highly dissociated oxygen plasma. Plasma was created in a glass Pyrex tube with an inductively coupled RF generator operating at a frequency of 27,12 MHz and an output of 200 W. The oxygen pressure was 75 Pa. The procedure is based on selective interaction of activated gaseous particles with the film coating. Selectivity of the etching process was achieved due to different oxidation probability of the polymer binder and TC pigments [19,20]. The method is frequently used to detect distribution and orientation of particles in polymer matrix [21,22]. The removal of the highest layers of polymer binder in UV-cured TC printing inks was completed in a couple of minutes. This way the top-laying TC pigment particles become visible on SEM micrographs.

Spectral reflectance was measured using a Lambda 950 UV-VIS-NIR spectrophotometer (Perkin–Elmer) employing a 150 mm integrating sphere under (8°:di) measuring geometry (diffuse geometry, specular component included) [22]. The printed sample was heated/cooled on the Full Cover water block (EK Water Blocks, EKWB d.o.o, Slovenia). The system was designed for cooling CPU's and graphic cards of power demanding computers. Only the basic part of this water-cooling engine was applied here, the water block, whereas the rest of the system was realized by thermostatic circulator which allows heating and cooling of the water block surface. The base plate is made of electrolytic copper lapped and polished to ±0,7 μm flatness. The water accelerates through very thin channels, made of acrylic material inside the plate. The copper base on the top is very thin, which gives very short distance for temperature to transfer from water through the plate and to the sample on it. The temperature of the copper plate surface was varied by circulation of thermostatically controlled water in channels inside water block. The applied thermostatic circulator allowed the water temperature to be adjusted up to tenth of degree accurately. The surface temperature of the water block was measured by infrared thermometer (Raytek MX2). It was confirmed that the surface temperature equals the temperature of the circulating water up to accuracy of at least ±0,5 °C. Above 80 °C electrically heated copper plate was applied, which temperature was controlled by microprocessor-based digital electronic controller (TLK 48, Technologic, Italy). Non-contact temperature measurements confirmed similar temperature accuracy as for the water block. Therefore the temperature of the sample placed in close contact on both heating/cooling apparatus was assumed to be accurate up to at least 1 °C.

The reflectance spectra were measured in three heating cycles differing in the temperature region in which the sample was measured. In each cycle the sample was heated from the lowest to the highest temperature and then cooled back to the lowest one. Between 19 and 35 °C the reflectance spectra were measured in 1 °C intervals but larger temperature difference was allowed (2 or 5 °C) elsewhere. Heating/cooling rate of about 0,5 °C/min was applied. The colorimetric parameters were calculated from the reflectance data using CIELAB colour space, under D50 illumination and 2° standard observer. Colour differences were calculated using the CIEDE2000 total colour difference formula [23].

## 3. Results and discussion

### 3.1. Physical properties

The size of the largest TC pigment particles in the three applied inks was ∼12 μm; this is the so-called grindometer value. The thickness of all UV-cured screen-printed layers was 11 ± 2 μm. Therefore the largest pigments should fill the entire thickness of dry layer.

Photomicrograph of the black TC ink obtained in bright filed is shown in Fig. 1a. Pigment particles have round geometry. Their size distribution was evaluated by image analysis of this micrograph. The result is shown in Fig. 1b. The particle size distribution is asymmetric with maximum at 4 μm, more precisely, the size of 26% of particles is between 3.5 and 4.5 μm. However, this is not the average particle size. Due to a broader population of larger particles, their average size is shifted to 5,0 μm. The largest particles are around 9.5 μm in diameter which is smaller than the grindometer value. It is very likely that transparent polymer envelopes of microencapsulated TC composite cannot be recognised as a part of TC capsules. Such an assumption would contribute a couple of μm to the wideness of the TC pigment particle. Then, the difference is the thickness of the capsule's shell. Practically the same size distribution was obtained from dark filed photomicrograph of the same TC ink. Similar results were obtained also for the blue and black TC inks.

The TC pigment particles were also monitored by SEM microscope. The surface of untreated samples shows some round-shaped features with few μm in diameter (Fig. 2a). These are TC pigment particles, i.e. the microencapsulated TC composite. The smallest particles seen on the surface could be some additive or possibly also some non-encapsulated composite. No boundary between particles and binder could be seen, which indicates that all particles are reasonably well covered by the binder. During exposure to weakly ionized oxygen plasma, the topmost material with the lowest oxidation probability is etched away first. This can be seen in Fig. 2b where the TC surface layer after 60 s treatment with plasma is shown. During the removal of the surface layer, the upper pigment particles become visible and their envelopes appear untouched. Removal of the covering binder changes the appearance of the sample but it still retains its original colour and responds well to temperature changes. However, at a longer exposure time the colour is lost and temperature response disappears. Typical example of such a sample is shown in Fig. 2c. The SEM micrograph of the sample surface after 180 s of exposure to oxygen plasma shows several pigment particles lying on the surface with extensively etched binder. Polymer envelopes of TC capsules are destroyed to a large extent. TC composite in such capsules is not protected from the environment and the colourization properties are irreversibly lost.

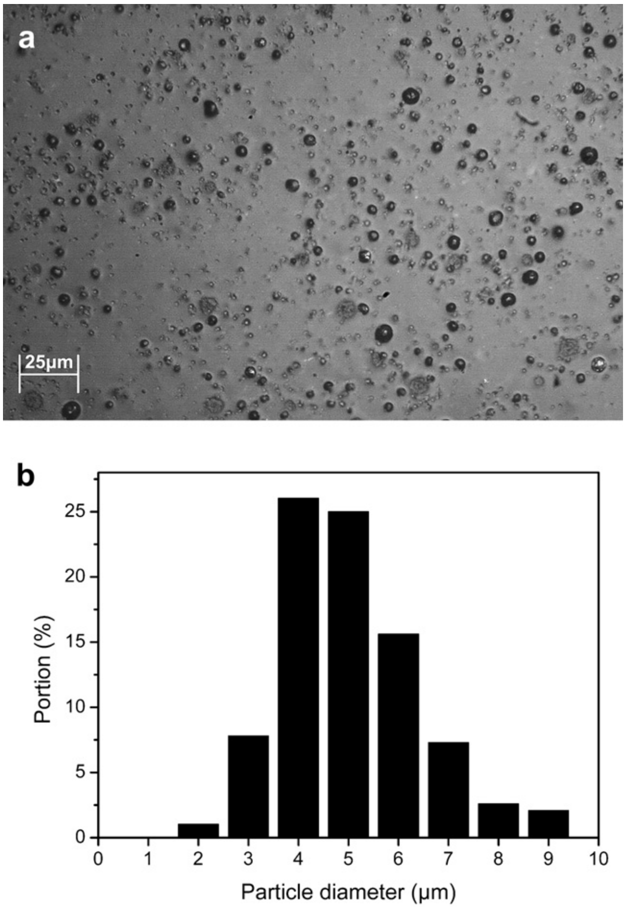

**Fig. 1.** Photomicrograph of the black TC sample in the bright field (a) gives wide asymmetric particle size distribution (b).

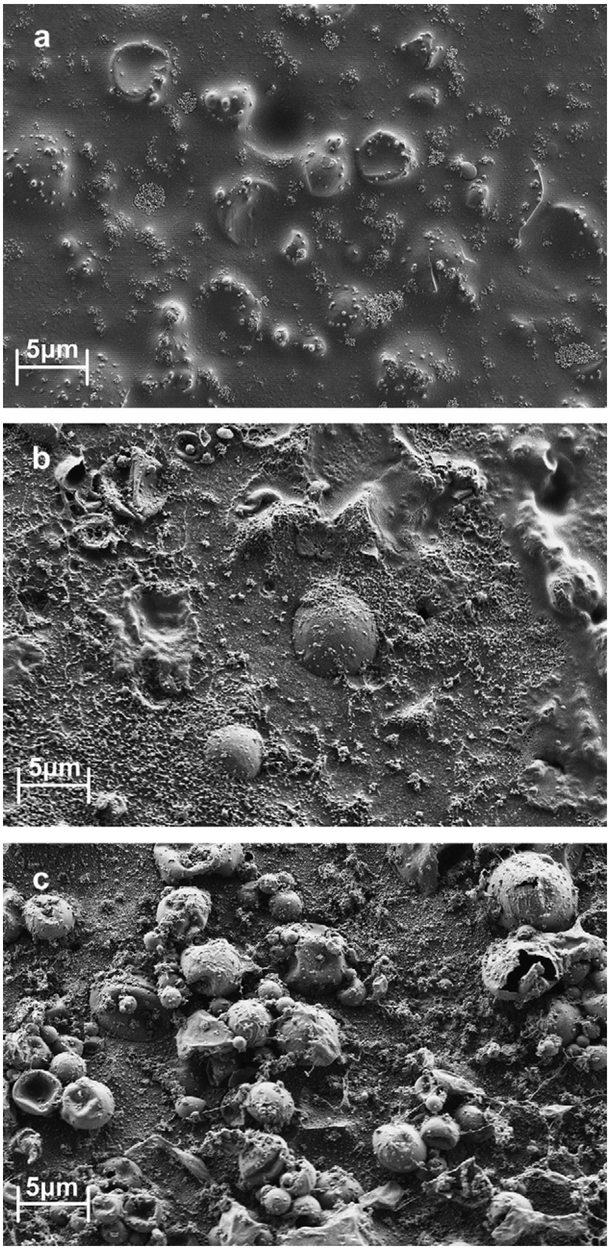

**Fig. 2.** SEM micrograph of the red TC screen-printed sample in untreated form (a) and after exposure to oxygen plasma for 60 s (b) and 180 s (c).

When coatings with conventional pigments are selectively etched by oxygen plasma, pigment particles appear on their surfaces at certain exposure and their size distribution can be evaluated. This is one of very few suitable direct methods for quantitative determination of the state of pigment dispersion in such coatings [21]. Conventional pigments are relatively stable against activated neutral oxygen radicals which are responsible for selective etching in weakly ionised oxygen plasma [19,20]. The situation is different in systems with TC pigments: the exposure time required to etch enough binder away is too long for particles' polymer shells. When they are destroyed, pigment particles change simultaneously so the method cannot be applied to evaluate the particle size distribution. However, this experiment shows that polymer envelopes are much more stable against selective etching than the binder itself; the binding energy of the molecular species in the polymer protecting capsule is much larger than it is inside the binder.

### 3.2. Colorimetric properties

The CIELAB values of the three TC samples were calculated applying measured reflectance spectra during heating from 15 °C up to 60 °C and cooling down to 15 °C. The results are shown in Fig. 3. TC samples lose their colour during heating and regain it during cooling. No abrupt change was observed-both processes are continuous. Decolourization is not complete even at the highest temperature applied in our experiment. All TC samples retain a yellow shade which differs from the uncoated paper (Table 1, *Yellowness*, total colour difference between the applied paper substrate and TC sample in fully decolourized form). This could be due to absorption and scattering of the binder/clear capsule system. The three inks applied here have the same binder and equally-sized TC particles with the same polymer envelope. In such conditions, *Yellowness* is a result of incomplete transparency of the TC composite inside capsules at high temperature. This effect is similar in the black and blue sample and somewhat larger in the red one.

The $a^*$, $b^*$ and $L^*$ values describe a path (a colour trajectory) in the CIELAB colour space (see Fig. 3). The trajectory obtained by heating is not completely equal to that obtained by cooling. The area of the surface defined by the two trajectories shows how similar the colour is when the sample goes through the heating/cooling cycle. When trajectories are identical, the corresponding area is zero. Larger area shows bigger differences between colours appearing on the sample when it is heated compared to when it is cooled. The values obtained for our samples are shown in Table 1. The largest area was obtained for the blue sample and the smallest for the black one. Therefore, the black TC sample describes the most similar colours whereas the blue one has apparently different dynamic colorimetric properties.

**Table 1**
Selected figures of dynamic colorimetric properties for the three TC inks: *Yellowness* and *Area* were calculated from data shown in Fig. 3. $T_{max}$, CIEDE2000$_{max}$ and *Spread* describe the temperature dependence of total colour difference between heated and cooled sample (Fig. 5): the temperature and the intensity of the maximum and the full-width at half-height of the peak, respectively. For details see the text.

| Sample | *Yellowness* | Area | $T_{max}$ (°C) | CIEDE2000$_{max}$ | *Spread* (°C) |
|---|---|---|---|---|---|
| Red | 4,3 | 81 | 27 | 22,7 | 6,2 |
| Blue | 2,9 | 247 | 27,5 | 36,8 | 6,7 |
| Black | 3,4 | 45 | 30 | 32,9 | 3,5 |

The reversible TC process depends on temperature which can be shown by change of lightness $L^*$ as a function of temperature (Fig. 4). When sample is heated, $L^*$ becomes higher. Most of the decolourization process is accomplished already some degrees above the activation temperature ($T_A$) where $L^*$ remains approximately the same with further increment of temperature. The reverse process occurs during cooling but at lower temperatures. The entire $L^*(T)$ curve has a form of a loop. Such a result shows that colour of a TC sample does not depend only on temperature, but also on the thermal history, i.e. whether the particular colour was reached during heating or during cooling. Therefore it is not possible to characterize the properties of such a sample in a selected time only by temperature. The TC system has memory-it is not possible to predict its output without knowing the path that it followed before the current state was reached. Such a phenomenon is called hysteresis. TC materials belong to several physical systems with hysteresis. It is colour hysteresis that describes the colour of a TC sample as a function of temperature.

Colour hysteresis describes temperature dependence of colour and should be represented in four-dimensional space or by two-dimensional graphs showing dependence of each component of colour on temperature separately. Fig. 4 shows such a graph for $L^*$-component of colour; similar loops were obtained also for $a^*$- and $b^*$-components. The area of colour hysteresis may also be

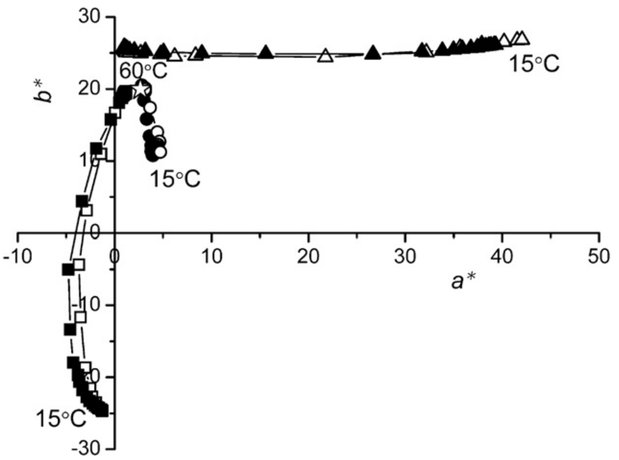

**Fig. 3.** Changing of CIELAB values of red (triangles), blue (squares) and black (circles) TC samples in the ($a^*$, $b^*$) plane at heating (solid signs) and cooling (open signs) in temperature region between 15 and 60 °C. The corresponding value of the bare substrate (uncoated paper) is shown by star.

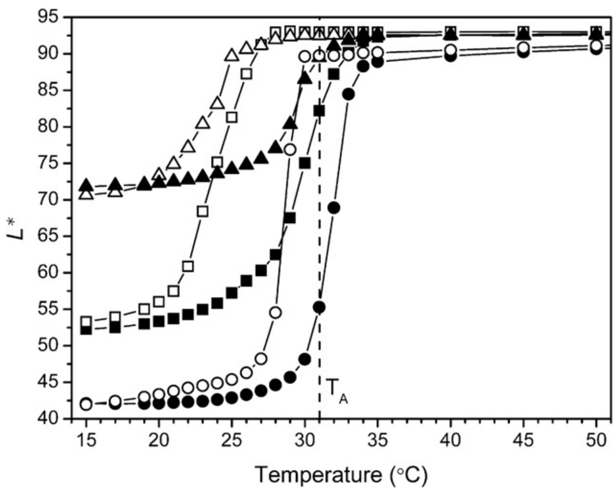

**Fig. 4.** CIELAB lightness $L^*$ of red (triangles), blue (squares) and black (circles) TC samples in dependence on temperature at heating (solid signs) and cooling (open signs).

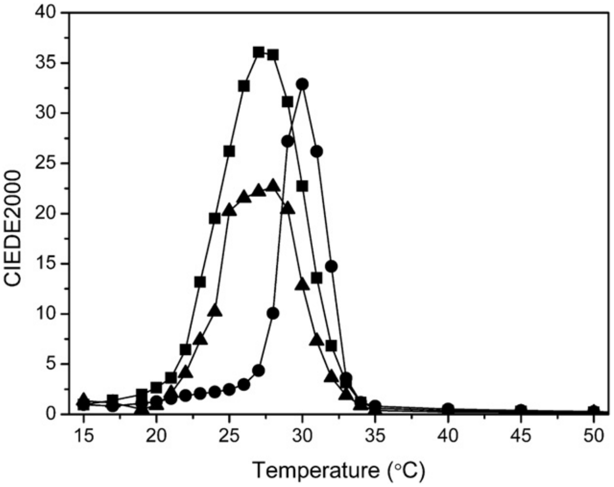

**Fig. 5.** Total colour difference between heated and cooled sample as measured for the red (triangles), blue (squares) and black (circles) TC samples as a function of temperature.

represented by the colour difference (CIEDE2000) between heated and cooled states of the same sample as a function of temperature. This is illustrated in Fig. 5. Our samples appear differently during the two reversible TC reactions (decolourization and colourization). Colour difference between heated and cooled sample reaches the largest values on the blue sample, peaks at similar temperatures on the blue and the red sample where it has approximately the same spread (full-width at half-height). The corresponding data are given in Table 1 ($T_{max}$, CIEDE2000$_{max}$, *Spread*). Higher CIEDE2000$_{max}$ shows larger colour change occurring at TC reaction and smaller *Spread* is due to larger colour gradient of the corresponding colour change. The largest colour change was obtained on the blue sample whereas the largest rate of colour change with temperature on the black sample.

**Table 2**
The characteristic temperatures of colour hysteresis for the three TC samples: initial achromic ($T_1$), final achromic ($T_2$), initial chromic ($T_3$) and final chromic ($T_4$) temperatures. See also Fig. 6.

| Sample | $T_1$ (°C) | $T_2$ (°C) | $T_3$ (°C) | $T_4$ (°C) |
|---|---|---|---|---|
| Red | 27,9 | 30,8 | 25,8 | 20,8 |
| Blue | 27,4 | 32,6 | 27,0 | 21,4 |
| Black | 30,1 | 33,6 | 29,7 | 27,3 |

The shape of colour hysteresis obtained for the three TC samples is typical for single-colour reversible thermochromism [8]. The curves obtained for the applied TC samples differ in temperatures where the loop starts and finishes, in its steepness and area. The characteristic temperatures were determined by the procedure illustrated on Fig. 6. The decolourization process is described by $T_1$ and $T_2$, the initial achromic and final achromic temperature and the reverse reaction by $T_3$ and $T_4$, the initial chromic and final chromic temperature, respectively. These temperatures can be determined from any two-dimensional graph showing colour hysteresis, $a^*(T)$, $b^*(T)$, $L^*(T)$ or $C^*(T)$. All these graphs give practically the same characteristic temperatures. They are collected in Table 2. The activation temperature, specified by the producer ($T_A = 31$ °C) does not correspond to any of these temperatures. It is located between $T_1$ and $T_2$, approaches well to $T_1$ in the black sample and to $T_2$ in the red one.

It is known from the literature that two metastable long-lived complexes are formed in a TC composite as a result of two competitive reactions, dye–developer and solvent–developer [10]. At low temperatures dye–developer interactions prevail which forms coloured dye–developer complexes. When at higher temperatures the solvent melts, solvent–developer interactions destroy the dye–developer complexes and TC composite transforms into its colourless state. Coloured complexes prevail at temperatures below $T_4$ and colourless complexes above $T_2$ regardless of thermal history of the sample. Between these two temperatures the system undergoes changes which depend on its thermal history. Between $T_1$ and $T_2$ decolourization occurs and between $T_3$ and $T_4$ the system regains colour. However, the temporal stability of the system between $T_3$ and $T_1$ might not be obvious. To analyse this, our TC samples were heated well above $T_2$ and then slowly cooled down just below $T_1$. Each sample was kept at this temperature for over 10 h (640 min). During this time several reflectance spectra were measured. After 640 min the

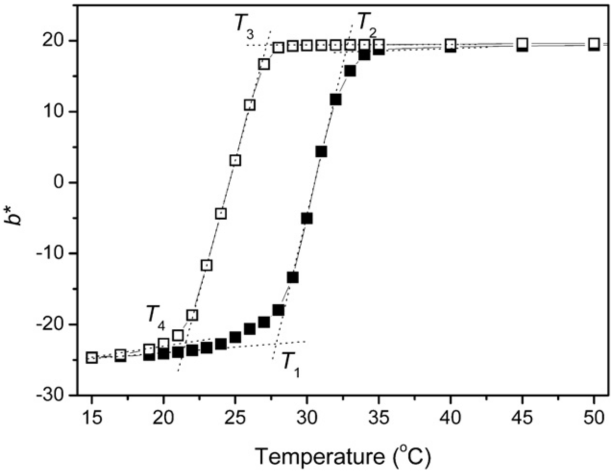

**Fig. 6.** Temperature dependence of the CIELAB $b^*$ values for the blue TC sample at heating (solid signs) and cooling (open signs). $T_1$ and $T_2$ are the initial achromic and final achromic temperatures describing decolourization process, whereas the $T_3$ and $T_4$ are the initial chromic and final chromic temperatures, describing coloration, respectively.

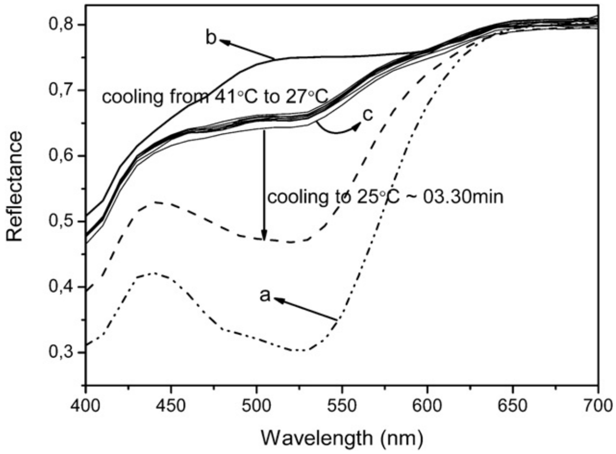

**Fig. 7.** Reflectance spectra measured to determine the stability of the decolourized state of the red TC sample at 27 °C. The reflectance of the colourized state at 27 °C was measured on heated sample (a) and the reflectance of the completely decolourized state at 41 °C (b). After cooling down to 27 °C, eight spectra were measured: after 0, 5, 10, 20, 40, 80, 160, 320 and 640 min at constant temperature (c). The reflectance of the sample slowly cooled to 25 °C after testing is also shown.

**Table 3**
Measuring parameters and results of colorimetric analysis of the three cycles: the lowest ($T_{\min}$) and the highest temperature ($T_{\max}$) and the total colour difference (CIEDE2000) between heated and cooled of the same sample at 15 °C.

| Cycle | $T_{\min}$ (°C) | $T_{\max}$ (°C) | CIEDE2000 | | |
|---|---|---|---|---|---|
| | | | Red | Blue | Black |
| A | 15 | 60 | 1,33 | 0,69 | 0,79 |
| B | 10 | 80 | 1,67 | 1,56 | 1,41 |
| C | 8 | 100 | 2,07 | 1,60 | 1,91 |

sample was slowly cooled and reflectance spectra were recorded. The temporal stability of decolourized state was measured at temperature little below $T_1$, i.e. 27 °C for the red and blue samples and 30 °C for the black one (compare with Table 2). The reflectance spectra recorded for the red TC sample are shown in Fig. 7. The examined state has stable colour during the entire tested time: the largest total colour difference (CIEDE2000) between any two measurements at constant temperature was 0,56 CIELAB units. When the temperature of tested sample was lowered, its colour path described the same colour hysteresis as measured without long time stability testing. Similar results were obtained for the blue and black TC samples.

In perfectly reversible process TC sample should return to the same colour after completing the whole heating/cooling cycle. Colour hysteresis of such a sample has a closed loop. The degree of reversibility of a TC change can be therefore evaluated by the opening of colour hysteresis loop at low temperatures, i.e. by total colour difference of a sample measured between heating and cooling at temperature well below the final chromic temperature ($T_4$). This value was applied to describe dependence of reversibility of the TC process on high temperatures. Three measuring cycles were applied, differing in the applied temperature region. Between successive cycles each sample was stored in a refrigerator for at least 12 h. Results obtained for the red, blue and black TC samples in the three measured cycles are given in Table 3. They show that the opening of the colour hysteresis depends on the applied temperature region: it increases with the highest temperature used for heating. This effect is approximately linear for the red and the black sample and is the largest for the red sample.

It should be pointed out here that the colorimetric properties of reversible TC process were tested up to the temperatures at which a short exposure should cause no long-lasting colour change (up to 140 °C, according to the producer data [24]). The high repeatability of dynamic colorimetric properties was reached by keeping each sample for several hours in refrigerator and by small temperature gradient applied for all measurements. This way the semi-permanent colour difference that remained in each cycle even well below final chromic temperature ($T_4$) was relaxed before starting the next cycle. Therefore no colour change of initial state was accumulated in successive cycles and each cycle is therefore independent on all others.

## 4. Conclusions

The colour of three, leuco dye-based TC inks of the same activation temperature were analysed. The pigments were of very similar size and the thickness of their protective polymer shell was is of the order of μm and are nearly equally stable against etching by oxygen plasma. It was shown that TC capsules are much more stable in oxygen plasma than the binder. Samples with damaged pigment capsules lose TC colour properties.

Leuco dye-based TC inks are coloured at low temperatures and transform into non-coloured state when heated. Their colour depends on temperature and on thermal history – this effect is known as hysteresis. The colours appearing on heating are in general not equal to those on cooling. The effect was measured by the surface area of colour hysteresis in a colour space. The colour difference observed on the same sample between heating and cooling at the same temperature peaks at different temperature, have different intensity and rate-of-change.

The shape of colour hysteresis can be characterized by four characteristic temperatures; two of them describe decolourization process that occurred by heating (initial achromic, final achromic) and the other two describe the repeated coloration at cooling (initial chromic, final chromic). The first (initial) temperature denotes where the corresponding competing reaction (achromic or chromic) starts whereas this reaction prevails at the second (final) temperature. The four temperatures therefore characterize the two chemical reactions producing colour loops. The three tested inks do not have the same characteristic temperatures. Activation temperature is the only parameter given by the producer that describes the dynamic colour of a TC ink. This temperature is higher than initial achromic and lower than final achromic temperature. Thus, no particular point of the whole TC process is described by the activation temperature.

Temporal stability of decolourized state at constant temperature was confirmed for more than 10 h when hysteresis cycle was stopped during cooling below initial achromic temperature but still above final chromic temperature. After the tested time period colour hysteresis continued practically the same path as without stability testing. The reversibility of the whole TC colour change, i.e. of the entire colour hysteresis, diminishes approximately linearly with the highest temperature applied at heating. In this testing, all temperatures were kept well below the highest temperatures recommended as acceptable by the producer. Small differences in the degree of this effect were obtained between tested inks. We may therefore conclude that the tested inks are not equally stable against higher temperatures.

All colour hystereses were measured applying small temperature gradient on samples with fully relaxed colour. It was proved that such conditions guarantee the high measurement repeatability required to quantify the dynamic colour properties of TC samples shown here.

The properties of TC inks shown here do not depend on physical properties of TC microcapsules. Dynamic colorimetric properties of a TC ink are suitable to describe by several parameters such as the area of colour hysteresis in colour space or by four characteristic temperatures of hysteresis loop. The opening of the loop at temperature well below the lowest of the four characteristic temperatures gives a measure of reversibility of the decolourization/colourization cycle. The analysis shown here provides a better description of the TC process in printed ink as the activation temperature and typical colour shade.

## Acknowledgements

Rahela Kulčar acknowledges the Centre of the Republic of Slovenia for Mobility and European Educational and Training programs – CMEPIUS for 4-months bilateral mobility grant.

Mojca Friškovec acknowledges the Slovenian Technology Agency for young researchers support, operation part financed by the European Union, European Social Fund. Operation implemented in the framework of the Operational Programme for Human Resources Development for the Period 2007–2013, Priority axis 1: Promoting entrepreneurship and adaptability, Main type of activity 1.1.: Experts and researchers for competitive enterprises.

Nina Hauptman acknowledges the Slovenian Research Agency for young researchers support.

## References

[1] Seeboth A, Lötzsch D. Thermochromic phenomena in polymers. Shawbury: Smithers Rapra Technology Limited; 2008.

[2] Homola J. Color-changing inks. http://www.screenweb.com/index.php/channel/6/id/1425/, http://www.mhest.com/spparticles/Color-changing-inks.pdf. Reprinted from McGraw-Hill Yearbook of Science & Technology; 2008.

[3] Williams CG. Colour change inks. Print & Paper Europe; Dec. 2002:22.

[4] Phillips GK. Combining thermochromics and conventional inks to deter document fraud. Proceedings of SPIE 2000;3973:99–104.

[5] Johansson L. Creation of printed dynamic images. Linköping Studies in Science and Technology; 2006. Thesis No. 1234. Norköpping.

[6] Maclaren DC, White MA. Dye–developer interactions in the crystal violet lactone-lauryl gallate binary system: implications for thermochromism. Journal of Materials Chemistry 2003;13:1695–700.

[7] MacLaren DC, White MA. Competition between dye–developer and solvent–developer interactions in a reversible thermochromic system. Journal of Materials Chemistry 2003;13:1701–4.

[8] Zhu CF, Wu AB. Studies on the synthesis and thermochromic properties of crystal violet lactone and its reversible thermochromic complexes. Thermochimica Acta 2005;425:7–12.

[9] MacLaren DC, White MA. Design rules for reversible thermochromic mixtures. Journal of Materials Chemistry 2005;40:669–76.

[10] Seeboth A, Lötzch D, Potechius E, Vetter R. Thermochromic effects of leuco dye studied in polypropylene. Chinese Journal of Polymer Science 2006;24:363–8.

[11] Seeboth A, Klukowska A, Ruhmann R, Lötzch D. Thermochromic polymer materials. Chinese Journal of Polymer Science 2007;25:123–35.

[12] White MA. Thermochromism in commercial products. Journal of Chemical Education 1999;76(9):1201–5.

[13] Aitken D, Burkinshaw SM, Griffiths J, Towns AD. Textile applications of thermochromic systems. Review of Progress on Coloration 1996;26:1–8.

[14] Burkinshaw SM, Griffiths J, Towns AD. Reversibly thermochromic systems based on pH-sensitive spirolactone-derived functional ink. Journal of Materials Chemistry 1998;8:267–83.

[15] Kito T, et al. Thermochromatic materials. US patent 4,421,560; 1983.

[16] Shibarashi Y, et al. Thermochromic materials. US patent 4,425,161; 1984.

[17] Kyoji T, et al. Method of reversible recording. EU patent EP 0 576 015 B1; 1993.

[18] Thermochromatic effects. Printcolor high performance inks. http://www.apcis.fr/ft/printcolor/documents/Thermochromatic_Effects.pdf.

[19] Mozetič M. Controlled oxidation of organic compounds in oxygen plasma. Vacuum 2003;71:237–40.

[20] Vesel A, Mozetič M, Hladnik A, Dolenc J, Zule J, Milošević S, et al. Modification of ink-jet paper by oxygen plasma treatment. Journal of Physics D: Applied Physics 2007;40:3689–96.

[21] Kunaver M, Klanjšek Gunde M, Mozetič M, Hrovat A. The degree of dispersion of pigments in powder coatings. Dyes and Pigments 2003;57:235–43.

[22] Klanjšek Gunde M, Kunaver M, Hrovat A, Cvelbar U. Bonding process efficiency and Al-flake orientation during the curing of powder coatings. Progress in Organic Coatings 2005;54:113–9.

[23] CIE Publication x015:2004. Colorimetry, 3rd ed. Vienna: CIE Central Buerau: 2004.

[24] Thermochrome Siebdruckfarben TCX. Technisches Merkblatt. Coates Screen: version Nr May 2006;6.